Journal Pre-proof

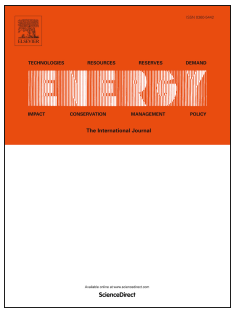

A time-series turbofan engine successive fault diagnosis under both steady-state and dynamic conditions

Yu-Zhi Chen, Elias Tsoutsanis, Chen Wang, Lin-Feng Gou, Theoklis Nikolaidis

PII: S0360-5442(22)02734-7

DOI: https://doi.org/10.1016/j.energy.2022.125848

Reference: EGY 125848

To appear in: *Energy*

Received Date: 28 May 2022

Revised Date: 19 October 2022

Accepted Date: 21 October 2022

Please cite this article as: Chen Y-Z, Tsoutsanis E, Wang C, Gou L-F, Nikolaidis T, A time-series turbofan engine successive fault diagnosis under both steady-state and dynamic conditions, *Energy* (2022), doi: https://doi.org/10.1016/j.energy.2022.125848.

This is a PDF file of an article that has undergone enhancements after acceptance, such as the addition of a cover page and metadata, and formatting for readability, but it is not yet the definitive version of record. This version will undergo additional copyediting, typesetting and review before it is published in its final form, but we are providing this version to give early visibility of the article. Please note that, during the production process, errors may be discovered which could affect the content, and all legal disclaimers that apply to the journal pertain.

© 2022 Published by Elsevier Ltd.

Journal Pre-proof

Yu-Zhi Chen: Conceptualization, Investigation, Methodology, Software, Writing - original draft.

Elias Tsoutsanis *: Conceptualization, Methodology, Visualization, Writing - review & editing.

Chen Wang: Methodology, Writing - review & editing.

Lin-Feng Gou: Methodology, Writing - review & editing.

Theoklis Nikolaidis: Methodology, Writing - review & editing.

Journal Pre-proof

Journal Pre-proof
Energy, Volume 263, Part D, January 2023, Article number 125848
DOI:10.1016/j.energy.2022.125848

A time-series turbofan engine successive fault diagnosis under both steady-state and dynamic conditions

Yu-Zhi Chen[1], Elias Tsoutsanis[2,*], Chen Wang[3], Lin-Feng Gou[4], Theoklis Nikolaidis[5]
[*] Corresponding author (elias.tsoutsanis@tii.ae)

ABSTRACT

In recent years there has been a growing interest in gas turbine fault diagnosis, especially under dynamic conditions, due to the evolving operating profile of gas turbines and the need to deploy computationally efficient and high-precision diagnostic solutions in real-time. One of the main challenges of fault diagnosis in real-time is the power imbalance between the compressor and turbine that occurs during transient operation. In addition, the heat soakage phenomenon characterizing the transient conditions has a substantial impact on the accuracy of the diagnosis. Finally, any sudden failure that might happen during transient operating conditions creates an additional challenge to fault diagnostics. The present study proposes a gas turbine diagnostic approach based on time-series measurements encapsulating steady-state and transient operating conditions. Specifically, the introduced novel approach is capable of quantifying the surplus/deficit of the power between the compressor and the turbine by utilizing the time-series data representing the observed deviations in the shaft rotational speed in order to determine the power balance in the shaft. The maximum diagnostic errors for constant fault and sudden failure are less than 0.006% during the dynamic maneuver. The results demonstrate and illustrate that the proposed method could effectively and accurately diagnose the severity of aero-engine faults at both steady-state and transient conditions. Therefore, this study has great potential for gas turbine practitioners since the diagnosis under transient conditions in real-

[1] School of Power and Energy, Northwestern Polytechnical University, Xi'an 710129, China
[2] Propulsion and Space Research Center, Technology Innovation Institute, Masdar City, PO Box: 9639, Abu Dhabi, United Arab Emirates
[3] Key Laboratory of Intelligent Control and Optimization for Industrial Equipment (Dalian University of Technology), Ministry of Education, Dalian 116024, China
[4] School of Power and Energy, Northwestern Polytechnical University, Xi'an 710129, China
[5] School of Aerospace, Transport and Manufacturing, Cranfield University, Bedford, UK

Published by Elsevier. This is the Author Accepted Manuscript issued with: Creative Commons Attribution Non-Commercial No Derivatives License (CC:BY:NC:ND 4.0).
The final published version (version of record) is available online at DOI:10.1016/j.energy.2022.125848. Please refer to any applicable publisher terms of use.

time can enhance the capability of engine online condition monitoring and improve the condition-based maintenance of gas turbine assets.

Key Words: Turbofan Engine Degradation; Time-series Fault Diagnosis; Real-time Engine Fault Monitoring.

Nomenclature

A	=	Area $[m^2]$
AW	=	Auxiliary work $[W]$
CP	=	Characteristic parameter
CW	=	Compressor work $[W]$
HP	=	High-pressure
I	=	Shaft inertia $[kg \cdot m^2]$
LP	=	Low-pressure
n	=	Number of measurements
N	=	Shaft rotational speed $[rpm]$
P	=	Pressure $[atm]$
PR	=	Pressure ratio
Q	=	Heat rate $[W]$
$RMSE$	=	Root mean square error
SP	=	Engine shaft surplus power $[W]$
T	=	Temperature $[Kelvin]$
TW	=	Turbine work $[W]$
U	=	Heat transfer coefficient $[W/(m^2 \cdot K)]$
W	=	Mass flow rate $[kg/s]$
X	=	Degradation index
Z	=	Measurements

Journal Pre-proof

Journal Pre-proof

Greek Letters

τ	=	Time constant $[s]$

Subscripts

a	=	Actual condition
c	=	Clean condition
E	=	Efficiency
F	=	Flow capacity
g	=	Gas flow
ht	=	heat transfer
in	=	Inlet
loc	=	Local component characteristic
m	=	Metal
out	=	Outlet

Journal Pre-proof

1. Introduction

The gas turbine engine is among the most important process engines for commercial and military aircraft [1]. Over the past years, there has been a dramatic development in gas turbine technology with more and more complex engine structures [2,3]. Gas path fault diagnosis is crucial to ensure the safety, economy, and reliability of aero-engine operations. Accordingly, a growing interest in gas path analysis (GPA) of gas turbine engines has been witnessed to guarantee effective condition-based maintenance. GPA is a gas path fault diagnosis technique that establishes the relationship between unmeasurable health parameters and measurable operating parameters [4]. GPA, established in 1969 by Urban [5], plays an essential role in the condition monitoring of gas turbine engines. As sudden failure has

dramatically impacted engine safety, real-time fault diagnosis is becoming a significant area of research in gas turbine engine condition monitoring.

The majority of aero-engine gas path analysis methods are based mainly on gas path measurements available from steady-state operating conditions [6]. In contrast, the gas path measurements obtained during transient conditions are mainly analyzed and processed offline, which cannot meet the requirement of online and real-time health monitoring. If the engine encounters a sudden fault during any transient maneuver, the steady-state gas path fault diagnostic system will not be able to respond promptly. In addition, engine component performance degradation will affect the compressor surge margin [7]. Therefore, real-time assessment of the compressor surge margin is crucial for safe control and operation of the engine transient process. Consequently, there is an urgent need to address the fault diagnosis in real-time under dynamic maneuvers for gas turbine engines on continuous feedback of gas path fault and improve the engine's emergency response capability. Until recently, little attention has been paid to the real-time monitoring of engines under transient conditions.

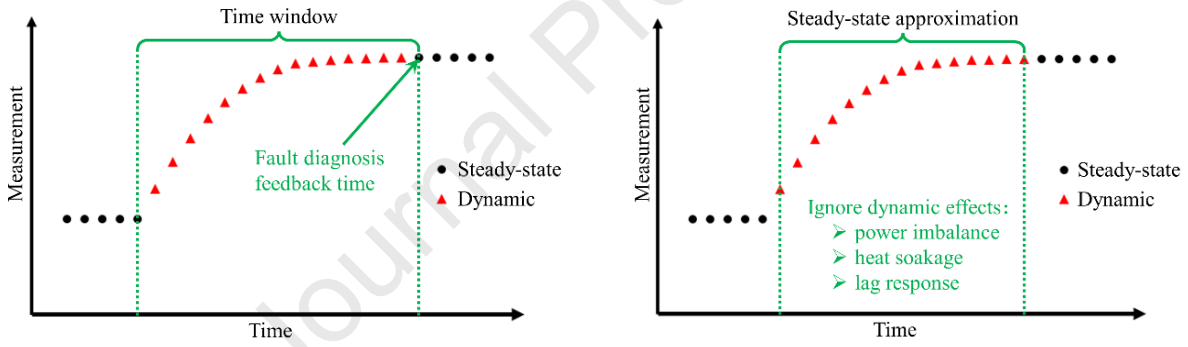

(a) Sliding window method (b) Steady-state approximation method

Fig. 1 Fault diagnosis methods at transient conditions.

In recent years, several attempts have been made to diagnose gas turbine degradation under both steady-state and transient conditions, where two different approaches have been proposed. The first one, the sliding window method, is to simulate the gas path measurements during the whole dynamic maneuver with estimated degradation and then compare them to the actual engine measurements from the monitoring system in order to iterate the predicted fault (Fig. 1 (a)). Li (2003) [8] developed a fault diagnosis method for turbofan engines under transient conditions based on the sliding window method. Ogaji et al. (2003) [9] conducted a gas turbine fault diagnosis based on artificial neural networks during a dynamic maneuver. Tsoutsanis et al. (2015) [10] proposed a fault diagnostic method by map tunning with selected sliding windows for the targeted gas path measurements, where the average prediction error is 0.15%. In the following two years, the GPA method has been further developed by Tsoutsanis et al. [11,12] to incorporate the

fault prognosis for gas turbines under dynamic conditions. Chen et al. (2022) [13] conducted an aero-engine fault diagnosis based on a sequential method under dynamic conditions. However, the above methods considered only soft degradation during a dynamic maneuver, which is the most common in gas turbines, but attention should be paid to the abrupt degradation scenarios in transient conditions.

The second method, the steady-state approximation method, considers time-series measurements independent. A steady-state fault diagnosis model is applied to each set of discrete measurements for both steady-state and dynamic conditions in the timeline (Fig. 1 (b)). Li and Ying (2020) [14] attempted to evaluate the degradation indices of a heavy-duty industrial gas turbine engine based on a steady-state approximation method for both steady-state and dynamic conditions. The diagnostic results were promising for the examined test cases, but the diagnosis accuracy might be compromised for other types of engines. The reason for this lies in the fact that the impact of transient conditions in the fault diagnosis, as expressed by a power imbalance, heat soakage, and lag response under dynamic conditions, has not been considered. Heavy-duty industrial gas turbine engines could ignore the aforementioned transient effects as they have the inertia of slow dynamic response. Still, they should be accounted for faster response gas turbine engines such as aero-derivative and aero-engines. Especially for engines with rapid transient maneuver capabilities and larger temperature and pressure variations in different operation conditions, the above method will be inappropriate, and the integrity of the diagnosis will be severely affected by transient effects. The power imbalance among different components on the same shafts and the heat soakage effect will greatly impact estimating the health parameters during dynamic conditions. Although the method could predict the health state in real-time, the predicted results will not be accurate, In such a situation.

The main challenge of fault diagnosis in real-time is the dynamic effect during transient maneuvers. Currently, fault diagnosis methods under transient conditions proceed either with the fault diagnosis after selecting a sliding window [2–5] or the steady-state approximation method without considering the dynamic effects such as heat soakage and power imbalance [14]. Therefore, it is of paramount importance for the condition-based maintenance of gas turbine engines to have a fault diagnosis algorithm that is capable of capturing the actual health state in real-time, even with sudden failure during dynamic operating conditions.

A time-series diagnostic method is proposed for gas turbine engines operating under both steady-state and dynamic conditions to address the gap mentioned above in the literature. The novelty of this study lies in the fact that we proposed a diagnostic method for transient conditions which could quantify the dynamic effects during transient

maneuvers at each time instant. The fault diagnosis captures the transient effect in the gas turbine in accordance with time series gas path measurement data. More specifically, the power imbalance between turbine and compressor is addressed by accounting for the shaft acceleration rate in order to determine both the surplus power under dynamic conditions and the power equality constraints for each shaft. The heat soakage effect during transient conditions could also be considered in the diagnosis model when previous measurements in the timeline are utilized to calculate the new metal temperature in the following timeline. In addition, the lag response that characterizes the transient conditions could be addressed by considering the first-order lag. Finally, as the measurements are successive, the sudden failure could also be diagnosed accurately during any time point of a dynamic maneuver. Based on the literature review, no publications have been found so far that could correctly diagnose the fault level in real-time under transient conditions. The main contributions of this study are summarized as follows:

1) A new real-time successive fault diagnosis method is proposed by considering the engine monitoring system under dynamic conditions.
2) The proposed algorithm considers transient effects on fault diagnosis based on time-dependence data.
3) The fault level of five engine components that experience degradation simultaneously could be reflected in real-time when new time-series data is transferred to the diagnostic system while the constant engine degradation is implanted.
4) In all previous research efforts, the sudden failure during dynamic conditions had a severity level that made it difficult to be monitored in real-time. This study could observe the sudden failure during a transient maneuver with excellent diagnosis accuracy.

The remaining part of the paper proceeds as follows: The second section of this paper will describe the methodology for the related methods. The third and fourth section of the paper deals with the application and the analysis, respectively. The final section summarizes the main findings and implications of this study.

2. Methodology

2.1 Assumptions

The methodology and test cases are based on the following assumptions since these will facilitate the comparison of the proposed method to a recently published benchmark method [14].

- Measurement noise/bias is ignored because there are mature methods for noise filtering and sensor verification [15,16]. Furthermore, rather than sensor-related issues, this research attempts to improve the performance of the diagnostic algorithm.
- The efficiency, flow capacity, and pressure ratio indices are used to quantify the fault level as health parameters. Furthermore, the pressure ratio index is assumed to be the same as the flow capacity index [17].
- All turbofan engine rotating components are experiencing degradation simultaneously. Moreover, any sudden failure will cause concurrent degradation of all engine components.

2.2 Turbofan Engine Performance and Degradation Modelling

2.2.1 Performance Modelling

Our previous publications have validated the steady-state and transient engine performance models [13,18] in the C # environment. Fig. 2 [13] presents the turbofan engine configuration with station numbering that includes a fan, a low-pressure compressor, a high-pressure compressor, a combustor, a high-pressure turbine, and a low-pressure turbine. The design point specification of the turbofan engine in concern is presented in Table 1. The turbofan engine measurements on-wing for fault diagnosis are listed in Table 2 [19].

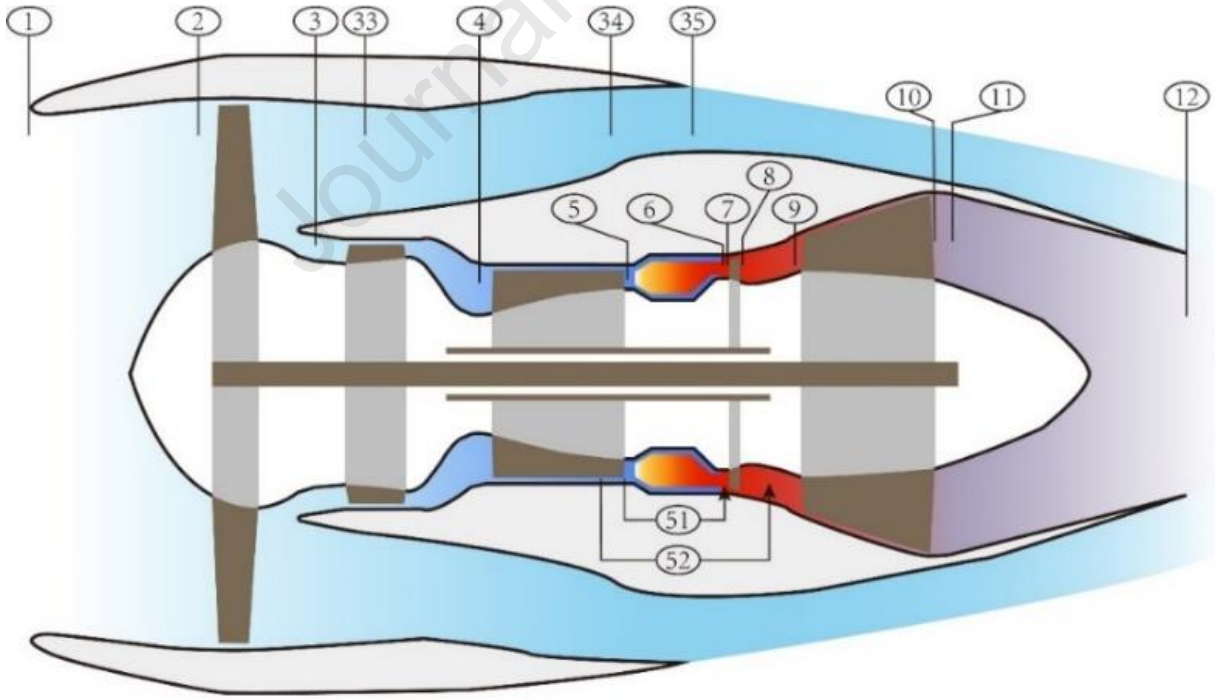

Fig. 2 Configuration of turbofan engine in concern and its station numbering [13].

Journal Pre-proof

Table 1 Turbofan engine design point specification.

Item	Symbol	Unit	Value
Flight Mach Number	MN	-	0.8
Flight Altitude	ALT	km	11
Intake Airflow Rate	W_{in}	kg/s	222
Burner Fuel Flow	W_{BFF}	kg/s	0.1876
Low Heating Value	LHV	MJ/kg	118.429
Engine Pressure Ratio	EPR	-	33.8
Engine Bypass Ratio	EBR	-	9

Table 2 Turbofan engine measurements on-wing [19].

No	Measurement	Symbol
1	Ambient pressure	P_1
2	Ambient temperature	T_1
3	Bypass inlet total pressure	P_{33}
4	Low-pressure compressor (*LPC*) exit total pressure	P_4
5	*LPC* exit total temperature	T_4
6	High-pressure compressor (*HPC*) exit total pressure	P_5
7	*HPC* exit total temperature	T_5
8	Low-pressure turbine (*LPT*) inlet total pressure	P_9
9	*LPT* inlet total temperature	T_9
10	*LPT* exit total pressure	P_{10}
11	*LPT* exit total temperature	T_{10}
12	Flight Mach Number	MN
13	*LP* shaft rotational speed	N_{LP}
14	*HP* shaft rotational speed	N_{HP}
15	Burner fuel flow rate	W_{Fuel}

2.2.2 Degradation Modelling

Normally, the performance of gas turbines is related to the performance of each sub-component [12,20]. Therefore, Eq. **(1)** defines the degradation index (X) which is related to the degradation of each component characteristic parameter[21,22].

$$X = \frac{CP_a}{CP_c} \quad \textbf{(1)}$$

where the subscript "a" and "c" represent the actual and clean conditions, respectively. If X is 1, it means that the engine is at a nominal clean condition where the denominator is the same as the numerator [23,24].

Table 3 [25] summarizes the health parameters relevant to the turbofan engine in concern. The 'Health State 1' refers to constant/smooth degradation of the engine in concern, whereas the 'Health State 2' refers to a more severe level of degradation, which is double that in 'Health State 1'. The magnitude of 'Health State 2' refers to a large bypass turbofan engine that has completed 6000 flight cycles [25]. The 'Health State 1' is also applied to the engine degradation level before sudden failure, whereas 'Health State 2' represents the engine degradation level after sudden failure.

Table 3 Degradation indices of turbofan engine [25].

Component	Symbol		Health Parameter	Health State 1	Health State 2 [25]
FAN	X_{FAN}	$X_{FAN,E}$	*FAN* efficiency index	-1.425 %	-2.85 %
		$X_{FAN,F}$	*FAN* flow capacity index	-1.825 %	-3.65 %
LPC	X_{LPC}	$X_{LPC,E}$	*LPC* efficiency index	-1.305 %	-2.61 %
		$X_{LPC,F}$	*LPC* flow capacity index	-2.00 %	-4.00 %
HPC	X_{HPC}	$X_{HPC,E}$	*HPC* efficiency index	-4.70 %	-9.40 %
		$X_{HPC,F}$	*HPC* flow capacity index	-7.03 %	-14.06 %
HPT	X_{HPT}	$X_{HPT,E}$	*HPT* efficiency index	-1.905 %	-3.81 %
		$X_{HPT,F}$	*HPT* flow capacity index	+1.285 %	+2.57 %
LPT	X_{LPT}	$X_{LPT,E}$	*LPT* efficiency index	-0.539 %	-1.078 %
		$X_{LPT,F}$	*LPT* flow capacity index	+0.2113 %	+0.4226 %

2.3 Benchmark Method

Nonlinear gas path analysis is widely used for model-based fault diagnosis, where the engine thermodynamic performance model may be defined by Eq. **(2)**. The iteration solver is applied to update the degradation index X during fault diagnosis in order to minimize the difference between the predicted measurements ($Z_{Predict}$) from the engine model and the actual measurements (Z_{Actual}) available from a service engine. In this study, the Newton-Rapson method [26] is chosen as the iteration solver for all the cases regarding performance simulation and fault diagnosis.

$$Z = f(X) \tag{2}$$

where Z denotes measurements of the engine, and X denotes the degradation indices of engine components.

The root mean square error ($RMSE$) defined by Eq. **(3)** [27,28] is selected to evaluate the convergence with a threshold of 1E-5 as the convergence criteria.

$$RMSE = \sqrt{\sum_{i=1}^{n} \frac{(Z_{Predict\ ,i} - Z_{Actual\ ,i})^2}{n}} \quad (3)$$

where n is the number of measurements.

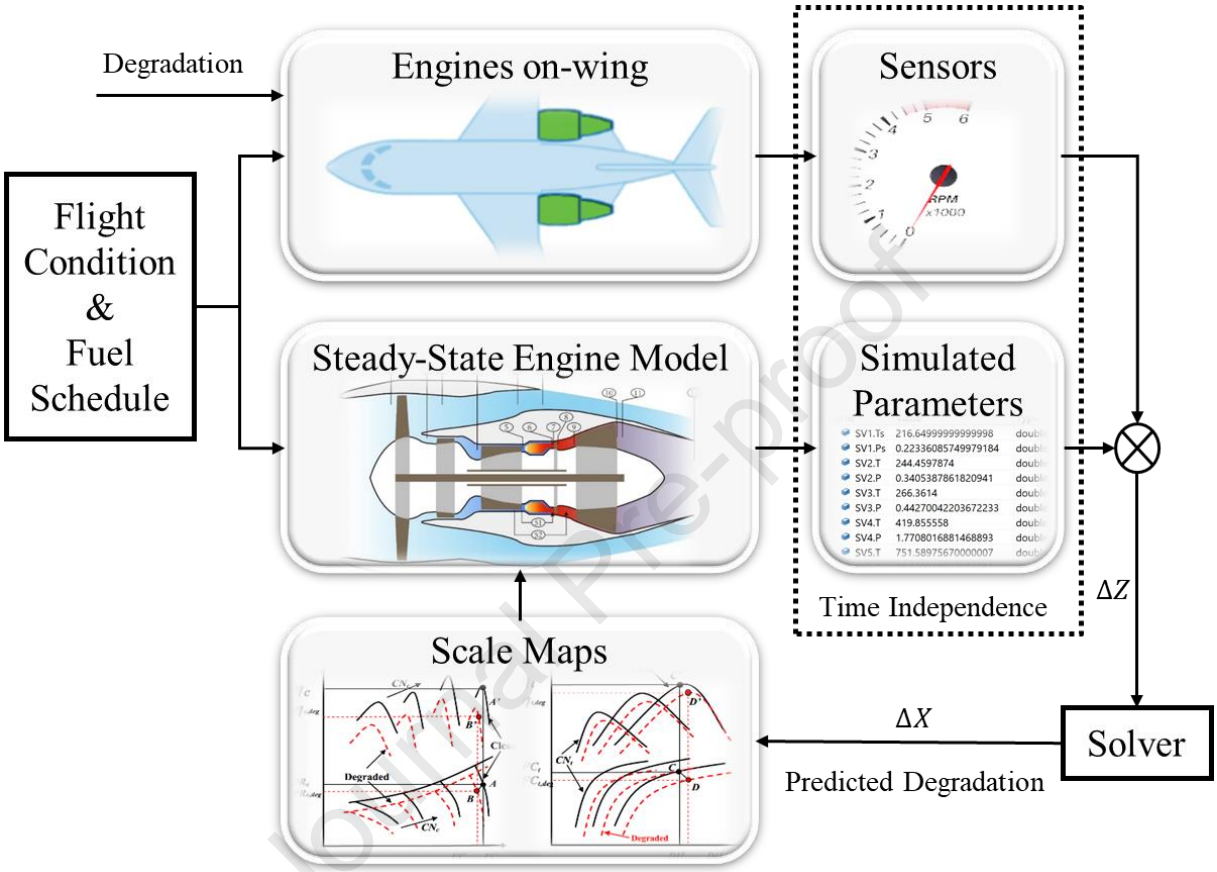

Fig. 3 Schematic of benchmark fault diagnosis method [13].

The method proposed by Li and Ying in 2020 [14] will be used as the "benchmark method" in this study. The schematic of the benchmark method is shown in Fig. 3 [13]. It is clear that the steady-state fault diagnosis model is characterized by time independence as the steady-state approximation is employed. The method will be applied to a high bypass ratio civil turbofan engine in order to generate some baseline diagnostic results.

The performance simulation and fault diagnosis processes are invoked in the same iteration loop. The iteration variables of the benchmark method are the ten degradation indices listed in Table 3 and the blocks with a purple color in Fig. 4. The convergence is checked based on compatibility shown in the blocks with blue color in Fig. 4. The detailed process is explained as follows:

The flight altitude, Mach Number, and inlet condition are known through on-wing measurements. Then, the fan inlet condition could be obtained by the intake model. It follows that the fan bypass pressure ratio could be calculated based on Eq. **(4)** [29] where P_{33} is a gas path measurement. As the fan inlet condition, shaft speed, and bypass pressure ratio are known, the fan outlet temperature and pressure at both core and bypass could be determined through the fan model [13].

$$PR_{FAN,BP} = P_{33}/P_2 \quad \textbf{(4)}$$

The LPC pressure ratio is obtained by Eq. **(5)** [30] where P_4 is a gas path measurement and P_3 could be determined from the fan model. Then, the LPC model calculation will follow as the pressure ratio, shaft speed, and inlet condition are known. It is worth noting that the core mass flow rate obtained in the LPC model is used to update the core flow and bypass flow rates in the fan model, which will also determine the bypass ratio. Moreover, the fan work is also updated according to the new bypass ratio.

$$PR_{LPC} = P_4/P_3 \quad \textbf{(5)}$$

The HPC pressure ratio can be obtained by Eq. **(6)** where P_5 and P_4 are gas path measurements. Then the HPC model could be used to calculate the outlet condition as the pressure ratio, shaft speed, and inlet condition are known.

$$PR_{HPC} = P_5/P_4 \quad \textbf{(6)}$$

As the HPC outlet condition is known, the burner outlet condition could be calculated as the fuel flow rate is also known. The mixture model is applied to calculate the HPT inlet condition. The HPT pressure ratio could be obtained by Eq. **(7)** where P_9 is gas path measurements and P_7 could be known from the mixture model after the combustor.

$$PR_{HPT} = P_7/P_9 \quad \textbf{(7)}$$

The LPT inlet condition could be obtained by the mixture after HPT. The LPT pressure ratio could be obtained by Eq. **(8)** [31] where P_9 and P_{10} are gas path measurements. Finally, two sets of duct and nozzle are applied to calculate main flow and bypass flow exhaust condition.

$$PR_{LPT} = P_9/P_{10} \quad \textbf{(8)}$$

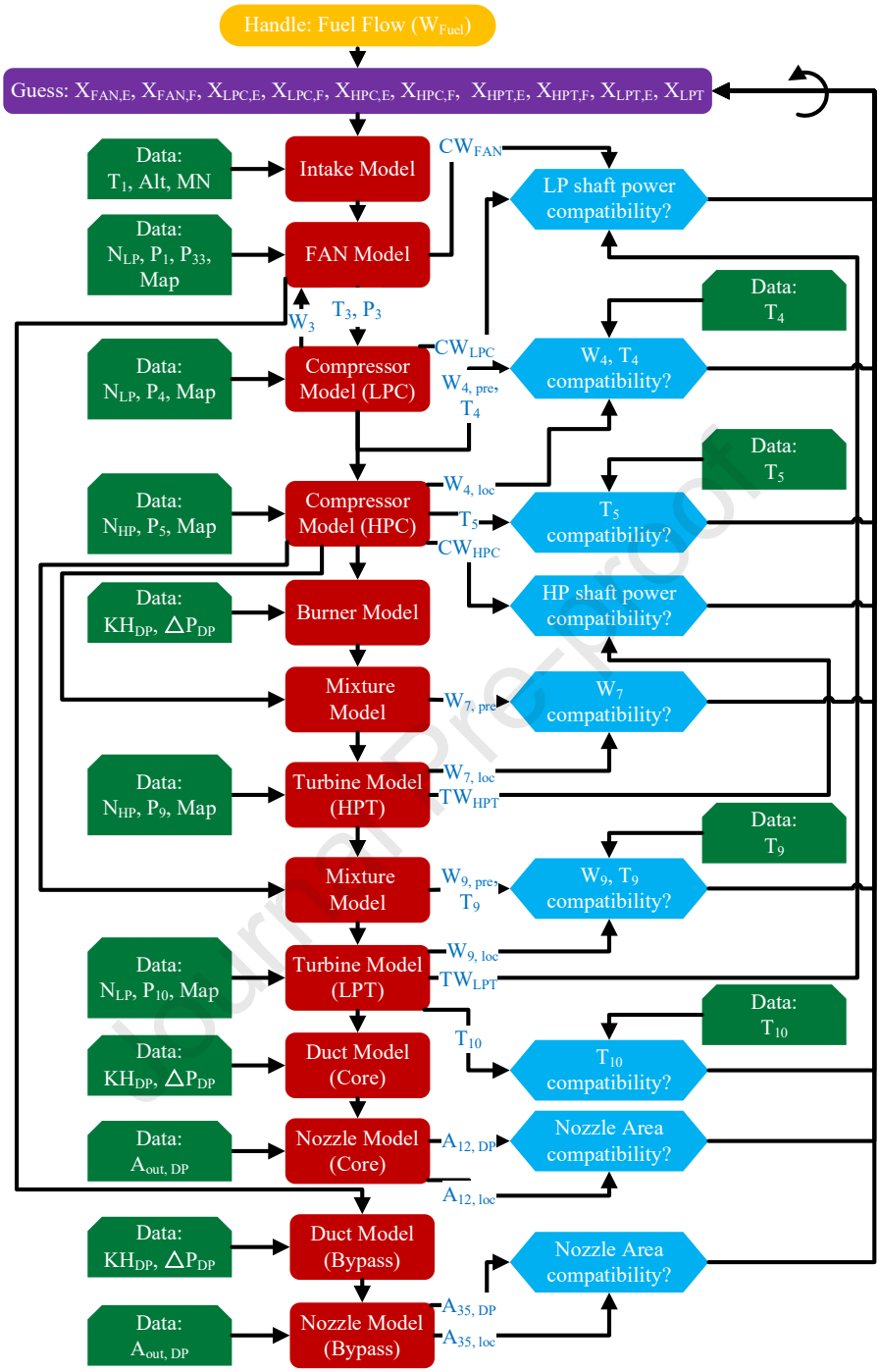

Fig. 4 Fault diagnosis based on steady-state model.

There are eleven convergence criteria in the diagnostic algorithm represented in blue blocks in Fig. 4. The convergence criteria could be classified into two categories. One set of convergence criteria is obtained from gas path measurements, including T_4, T_5, T_9, and T_{10}. The other set of convergence criteria is required to satisfy the mass flow compatibility, shaft power balance, and design nozzle area at the design point. It is worth noting that the LP and HP

236 shaft power compatibility in blue blocks means that the turbine work has to be equal to the compressor work plus any
237 auxiliary work at all times, as the steady-state approximation fault diagnosis method is employed. This is one of the
238 main assumptions of the benchmark method that may lead to diagnostic errors since the surplus power during dynamic
239 conditions is ignored. Another source of uncertainty is the assumption that the typical phenomenon of heat soakage
240 and lag response during dynamic conditions is ignored when the steady-state model is implemented. In such a
241 condition, diagnostic accuracy may be compromised.

242 **2.4 Proposed Method**

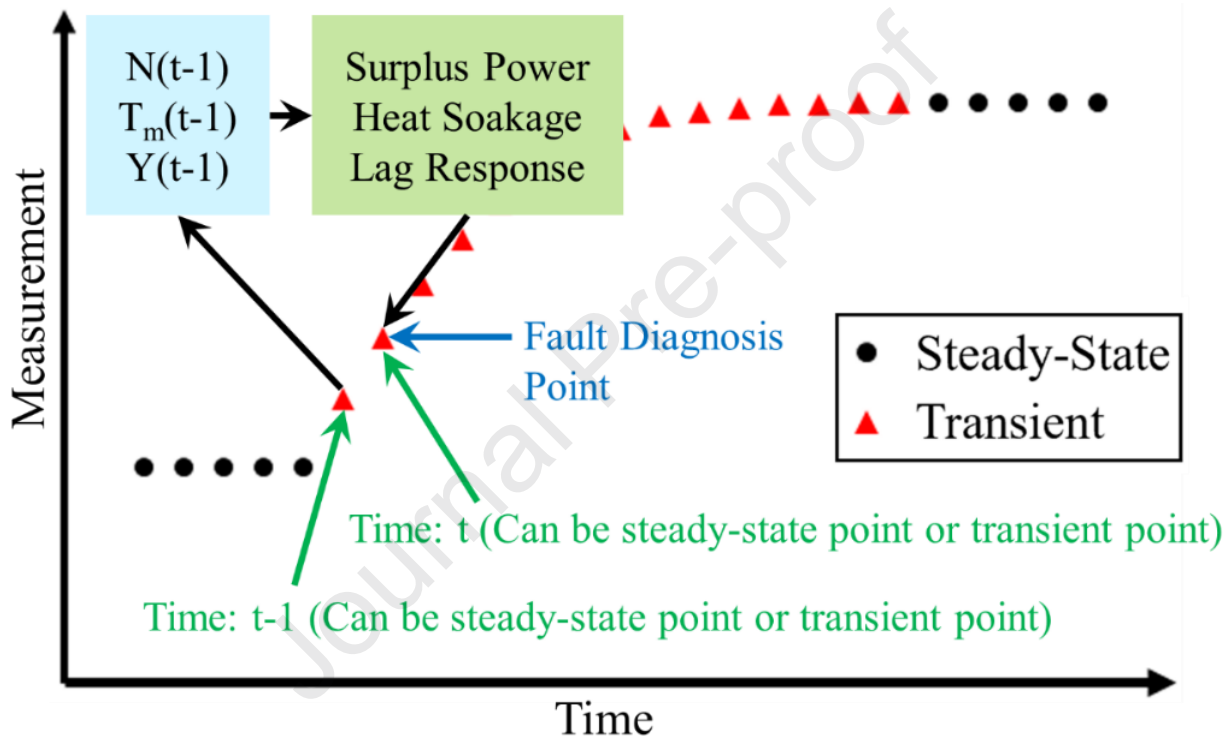

243

244 **Fig. 5 Schematic of proposed fault diagnosis method.**

245 The benchmark method may be sufficient for slow transient maneuvers which characterize heavy-duty industrial
246 gas turbines as the steady-state approximation is employed in their study. However, the performance of the benchmark
247 method is limited in transient conditions if the power imbalance among shaft, heat soakage, and lag response are not
248 considered. This study intends to diagnose the health of a civil turbofan engine with time-series data during steady-
249 state and transient conditions. The transient effect could not be ignored for the turbofan engine in concern as it exhibits
250 a fast and dynamic response. The schematic of the proposed method is demonstrated in Fig. 5, where shaft speeds
251 derive the surplus power during dynamic processes among adjacent measurement steps in the diagnostic system for
252 the consideration of shaft power compatibility in Fig. 4. Moreover, the heat soakage is also considered in the engine

sub-models to represent the heat transfer between gas and engine metal during the transient maneuver for the temperature compatibility check in Fig. 4. the first order lag is selected in this study to represent the lag response of sensor property in Fig. 4 under dynamic conditions. It is clear that the measurements are time-dependent in the proposed method, where the surplus power, transient heat transfer, and lag response are needed to be considered in consecutive time steps, which are highlighted in the green block in Fig. 5. In addition, the shaft model also takes lag response into account to capture the dynamic response with increased precision. Although the two red points under dynamic conditions are selected to illustrate the new method in Fig. 5, the proposed method is also suitable for steady-state conditions.

2.4.1 Rotor Dynamics

Gas path measurements could not directly monitor the surplus power among each shaft. As the engine shaft speed is monitored in time-series, the rotor acceleration rate could be derived through the deviation of shaft speed in finite time steps by Eq. **(9)** [32,33].

$$\frac{dN}{dt} = \frac{N(t+\Delta t) - N(t)}{\Delta t} \tag{9}$$

In such a condition, the surplus power (SP) could be calculated by Eq. **(10)** [34,35] by rotor acceleration rate, shaft speed, and shaft inertia (I).

$$SP = \frac{4\pi^2}{3600} \cdot I \cdot N \cdot \frac{dN}{dt} \tag{10}$$

Then, the power balance among each shaft could be obtained by **(11)** [36,37]. The equation is tenable for both steady-state and dynamic conditions where the SP is zero during the steady-state condition. Hence, the proposed method could satisfy the shaft power compatibility when surplus power is considered for both steady-state and dynamic conditions in a more coherent fashion than the benchmark method.

$$TW = SP + CW + AW \tag{11}$$

where TW is turbine work, CW is compressor work, and AW is auxiliary work for power offtake.

2.4.2 Heat Soakage

During transient maneuvering, changing gas temperature in a turbofan engine will affect the engine metal temperature. This phenomenon is called heat soakage and is not considered in the steady-state fault diagnosis of the benchmark method.

The heat soakage is considered in the dynamic engine model in the proposed method. The heat transfer between gas flow and engine metal is obtained by Eq. **(12)** with exponential decay [38].

$$Q = U_{ht} \cdot A_{ht}(T^{b}_{g,k+1} - T_{m,k}) \cdot (e^{-\Delta t/\tau} - 1) \tag{12}$$

where Q is heat rate, U_{ht} is heat transfer coefficient, A_{ht} is the effective contact surface, $T^{b}_{g,k+1}$ is the gas temperature in the current step before considering heat soakage, $T_{m,k}$ is the metal temperature in the previous step, Δt is the time step, and τ is the time constant.

The heat transfer coefficient is calculated as follows:

$$U_{ht} = \frac{1}{\frac{1}{FC} + \frac{l_{eff}}{k_m}} \tag{13}$$

Additionally, the time constant is determined by Eq. **(14)**.

$$\tau = \frac{c_m \cdot W_m}{U_{ht} \cdot A_{ht}} \tag{14}$$

where W_m is the effective mass of engine component, c_m is the specific heat of the engine material.

The change of engine metal temperature (dT_m) could be obtained by Eq. **(15)**.

$$\frac{dT_m}{dt} = \frac{Q}{c_m \cdot W_m} \tag{15}$$

The metal temperature of the engine component in the current step ($T_{m,k+1}$) could be obtained as follows:

$$T_{m,k+1} = T_{m,k} - dT_m \tag{16}$$

The change of gas enthalpy (ΔH_g) when considering the heat transfer could be determined by Eq. **(17)**.

$$\Delta H_g = \frac{Q}{W_g} \tag{17}$$

where W_g is the mass flow rate of gas.

The gas enthalpy at the current step with the consideration of heat soakage ($H_{g,k+1}$) could be obtained as follows:

$$H_{g,k+1} = H^{b}_{g,k+1} + \Delta H_g \tag{18}$$

where $H^{b}_{g,k+1}$ is gas enthalpy at current step before considering heat soakage.

The gas temperature at the current step with the consideration of heat soakage ($T_{g,k+1}$) could be determined by Eq. **(19)**.

$$T_{g,k+1} = GasProp_{[H,P]}(H_{g,k+1}, P_{g,k+1}, FAR, WAR) \tag{19}$$

2.4.3 Lag Response of Engine Shafts

The time delay phenomenon of the engine shafts during transient maneuvering is represented using the first-order lag. As $N_{out}(s)$ is measured through an on-wing monitoring system, the $N_{in}(s)$ could be derived by Eq. **(20)** [39,40] for the engine model.

$$\frac{N_{out}\ (s)}{N_{in}(s)} = \frac{1}{\tau \cdot s + 1} \tag{20}$$

where τ is the characteristic time, $N_{out}(s)$ is the input with delay and $N_{in}(s)$ is the input value without delay.

3. Application and Analysis

Four case studies are examined in this paper. In order to make a direct comparison between the proposed and the benchmark methods [14], the same computer environment is used. To be more specific, a personal computer with Intel(R) i7 CPU @2.90GHz and 16 GB RAM is used to evaluate the computational time of the diagnostic process for all case studies. The four cases are specified as follows:

Case 1. This case study aims to evaluate the effectiveness of the benchmark diagnostic method [14] when the engine gas path measurements represent dynamic operating conditions without consideration of heat soakage.

Case 2. The measurements in this case study represent the dynamic performance with the effect of heat soakage included. This case study aims to investigate the effectiveness of the benchmark diagnostic method [14] for diagnosing the health of the engine from transient measurements by taking into account the heat soakage phenomenon in order to set a baseline diagnostic data set that will be further used for comparing it with the proposed method.

Case 3. This case study demonstrates and illustrates the proposed method's advantage compared to the baseline diagnostic results from Case 2, which implemented the benchmark method [14].

Case 4. While the previous three case studies tested the diagnostic results under constant fault levels during a transient maneuver, this case study is designed to demonstrate the capability of the proposed method to deal with sudden failure during transient operation.

The first three cases have a constant degradation level called 'Health State 1' as shown in Table 3 [25]. In Case study 4, we inject the degradation level denoted as 'Health State 1' between [0-3) s and 'Health State 2' between [3-15] s with the sudden failure initiated at the time mark of 3.0 s.

3.1 Case 1: Benchmark Method - Transient Measurements without Considering Heat Soakage

As mentioned in the methodology, the benchmark method [14] did not take into account the surplus power in the fault diagnosis during dynamic conditions. This may be true as the focus of that study was a heavy-duty industrial gas turbine engine. Due to its large shaft inertia, the transient maneuver for heavy-duty gas turbine engines is relatively slower than other gas turbines (i.e., aero-derivative engines and turbofans). However, such an assumption will compromise the diagnostic performance of other gas turbines.

Fig. 6 (top) demonstrates an acceleration fuel schedule with a 0.1 s time step during a dynamic maneuver for the turbofan engine in concern. It is well known that the power balance between compressor work and turbine work will not be satisfied during the transient maneuver. As shown in Fig. 6 (middle), the maximum surplus power obtained from the power imbalance between the compressor and turbine is close to 320 kW during the maneuver for both *LP* and *HP* shafts. The maximum difference between compressor work and turbine work is 5.3% and 3.0% for *LP* and *HP* shaft in Fig. 6 (bottom), respectively. Therefore, if the surplus power is ignored, the relative error will propagate to the diagnostic results. It follows that the larger the surplus power, the less accurate the diagnostic results will worsen in steady-state approximation.

The average computation time for diagnosis with the benchmark method is 0.2024 s. Fig. 7 presents the diagnostic results based on the benchmark method. It is apparent from this figure that the surplus power impacts the accuracy of the diagnosis. The error of the diagnosis keeps increasing until approximately the 3 s mark, where the maximum prediction error is observed. Then, the prediction error of health parameters decreases as the surplus power falls off. In such a condition, the benchmark method will lead to fluctuation of the diagnostic results and may set a false alarm of sudden engine degradation. Moreover, the faster the variation of the fuel schedule is, the larger the surplus power and the bigger the prediction errors are going to be. The average prediction error of all ten health parameters during the transient maneuver is shown in Fig. 8. Although the average maximum prediction error of ten health parameters

hovers at 1.4265% in Fig. 8, the maximum prediction error during the dynamic maneuver is 6.3396 % at 2.6 s for $X_{FAN,E}$. Such a prediction error may lead to inaccurate diagnosis.

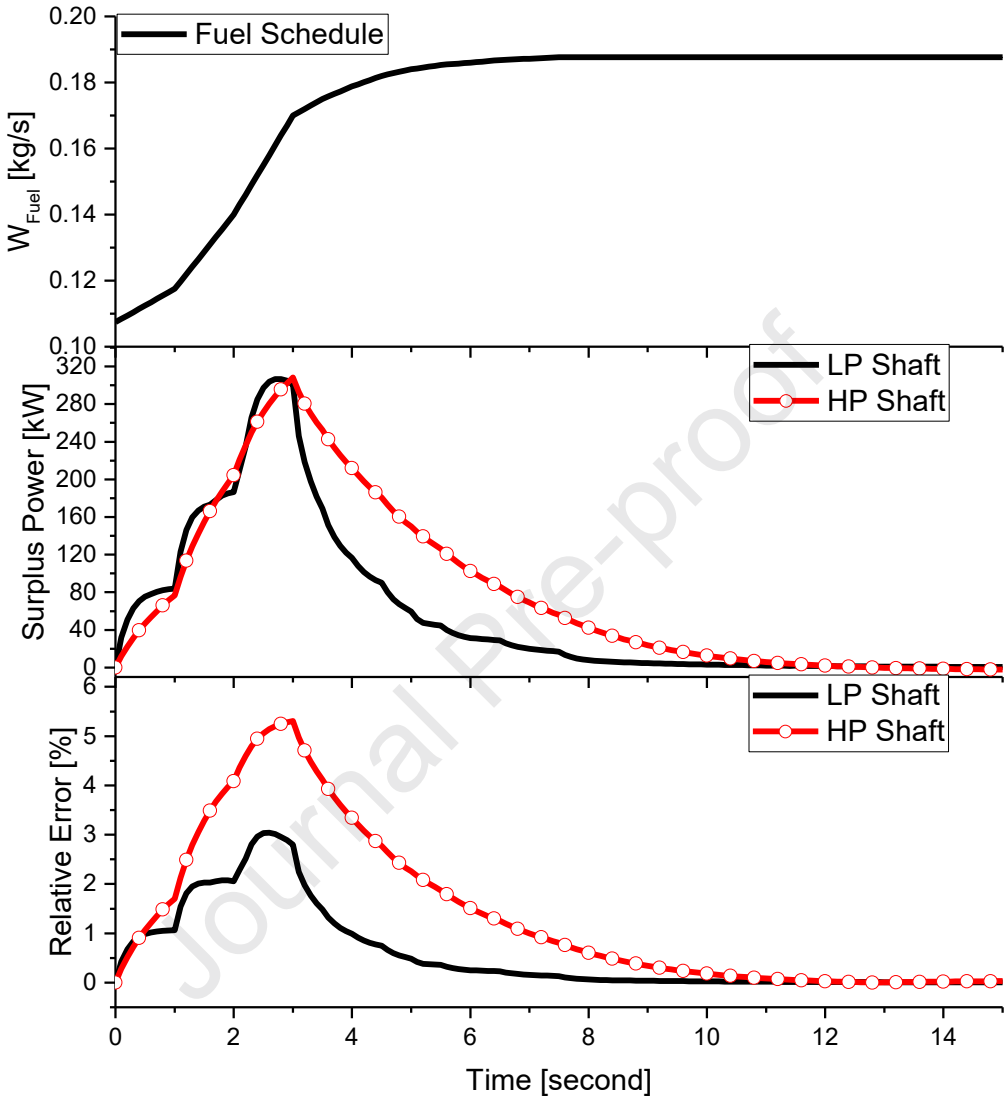

Fig. 6 Fuel schedule and power imbalance between *CW* and *TW* during a transient maneuver.

In summary, the benchmark method could be beneficial if the surplus power is negligible. This typically happens when there is a slow variation of fuel flow rate with respect to time during a transient maneuver. In other cases, the benchmark method will significantly fluctuate its diagnostic results. Consequentially, the benchmark method cannot monitor the engine health state in real-time when each set of measurements is recorded. Thus, such a method is not capable of monitoring the sudden engine failure that a bird strike may cause.

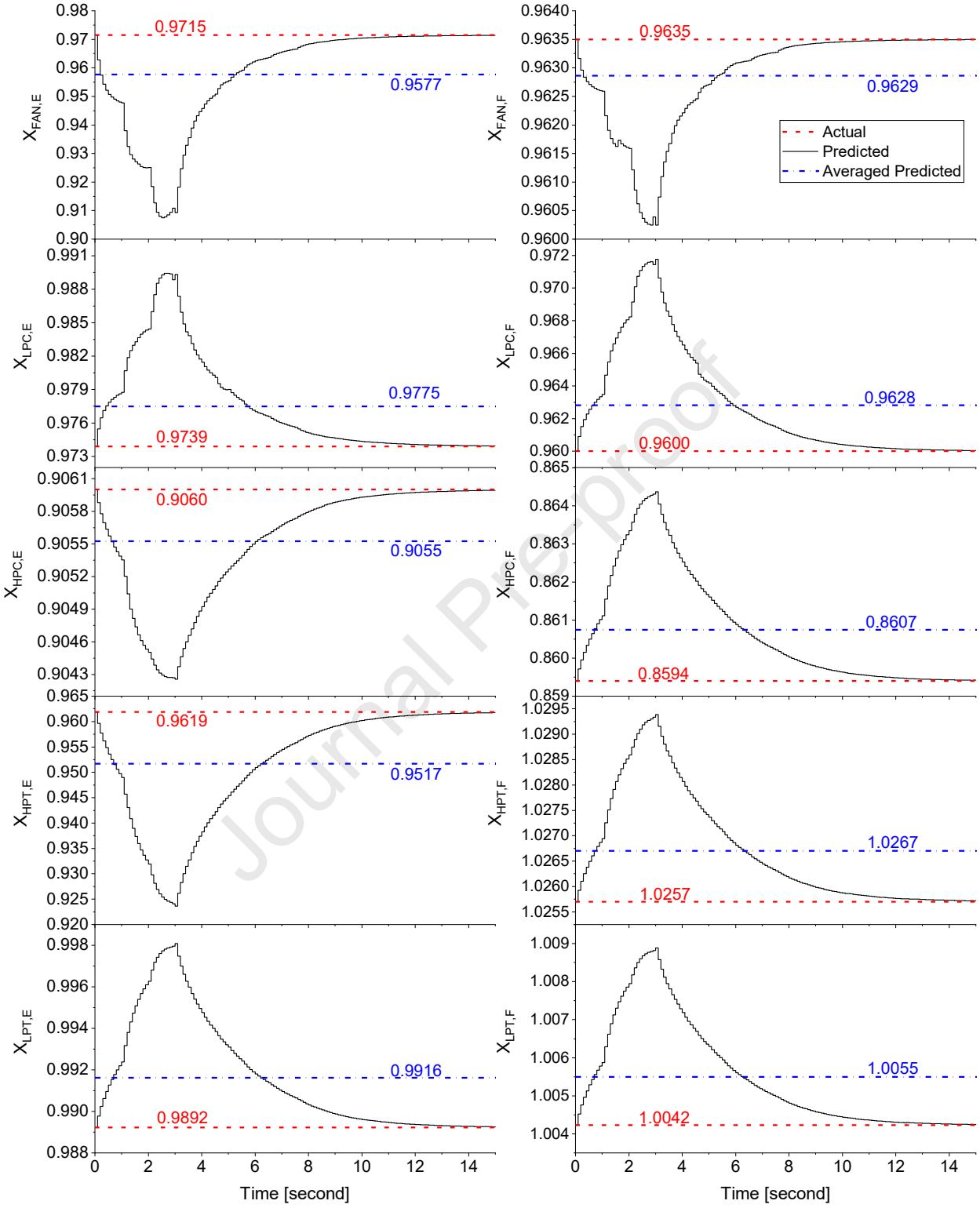

Fig. 7 Predicted health parameters during a transient maneuver.

Journal Pre-proof

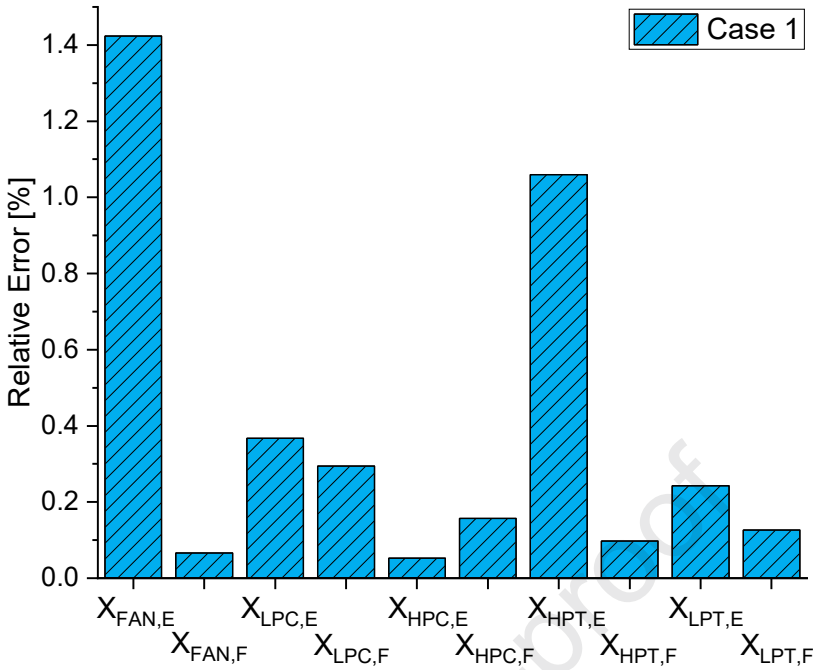

Fig. 8 Average relative error of health parameters during a transient maneuver.

3.2 Case 2: Benchmark Method - Transient Measurements by Considering Heat Soakage

During dynamic operating conditions, the gas turbine is not only facing power imbalance among shafts but also experiences heat transfer between gas and engine components. Fig. 9 presents the effect of heat soakage on exhaust gas temperature with time during a transient maneuver with and without considering heat soakage. It is evident that heat soakage impacts the gas path measurement of the exhaust temperature by delaying its increase in comparison with the case where heat soakage is ignored, as seen in Fig. 9. If the engine is faced with a slam transient maneuver, the predicted engine health parameters are likely to be affected.

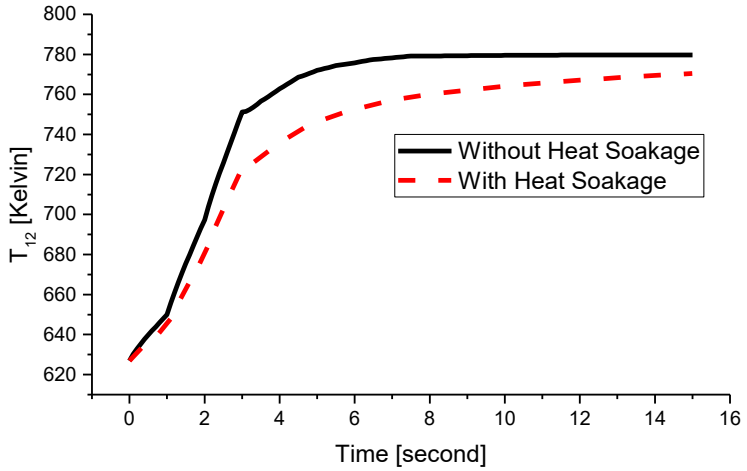

Fig. 9 Effect of heat soakage on exhaust gas temperature.

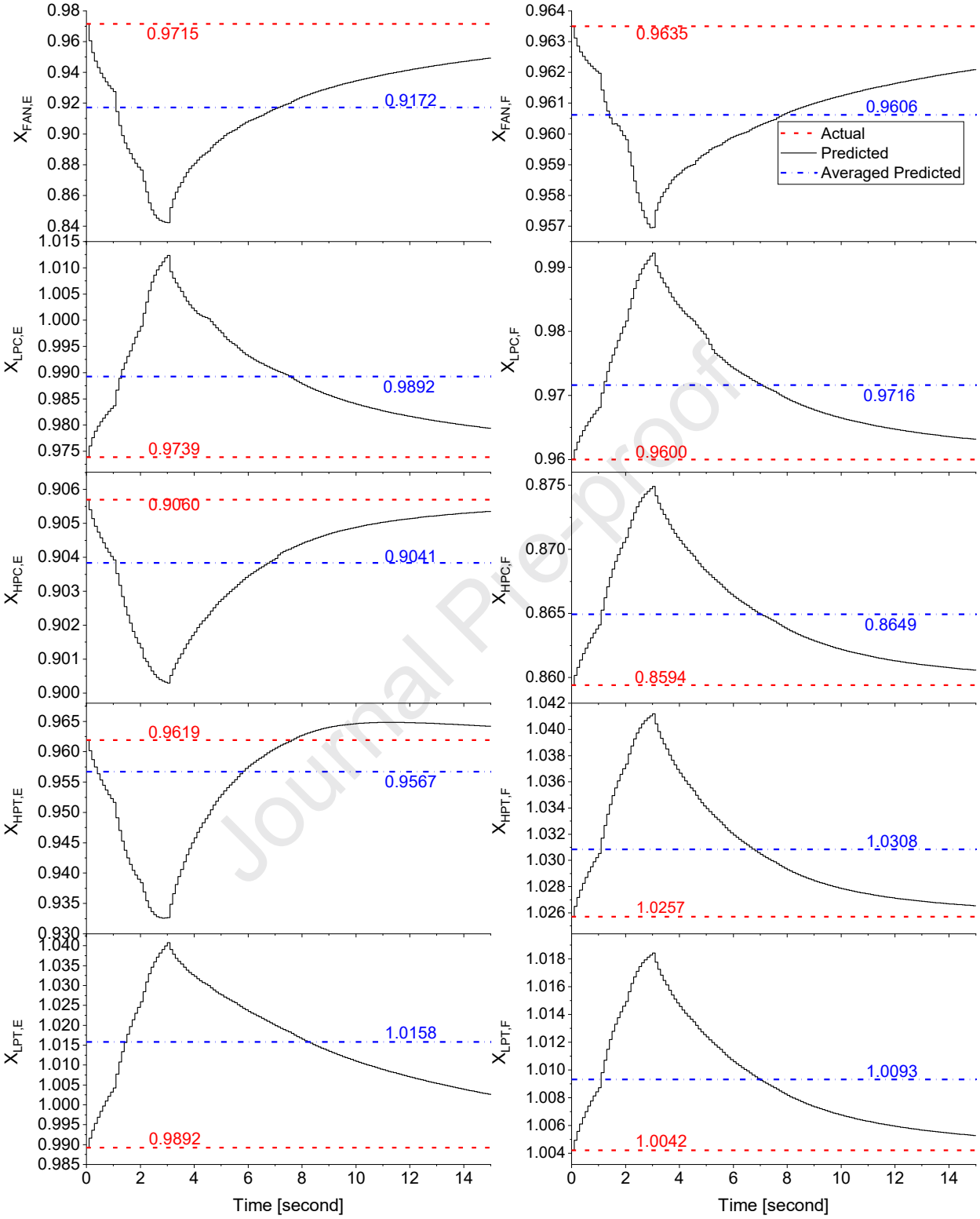

Fig. 10 Predicted health parameters during a transient maneuver.

The average computation time for diagnosis is 0.1997 during the 15 s maneuver, where the benchmark method has been implemented. It can be seen from the plot in Fig. 10 that the estimated degradation indices have a relatively

higher deviation from the actual health state when compared with Case 1. Apart from the HPT efficiency degradation index, the heat soakage phenomenon will increase the prediction error when considering the heat soakage in transient measurements. The surplus power will lead to over-prediction of the HPT efficiency degradation, while the heat soakage will under-predict the HPT efficiency degradation. Fig. 11 provides the summary of the average prediction error for ten health parameters. The maximum average error of the benchmark method has increased from 1.4265 % in Case 1 to 5.8738 % in Case 2 when the transient measurements consider heat soakage. Moreover, the maximum error during the entire transient maneuver is 13.3647 in Case 2 at 3.0 s for $X_{FAN,E}$. The consideration of heat soakage in the engine measurements will delay the prediction of the maximum degradation for all ten degradation indices. Ignoring the heat soakage during transient diagnosis will impact the prediction accuracy during transient conditions.

The results of this case study provide important insights into the applicability of the benchmark method for engine transient maneuvers. It becomes clear that using transient measurements in a steady-state approximation fault diagnostic system will have noticeable prediction errors during dynamic operating conditions. Moreover, the shift of diagnostic results is possible to raise a false alarm. If the diagnostic system dispatches frequent false alarms, the fault diagnostic program's confidence will be significantly compromised from an operation and maintenance perspective.

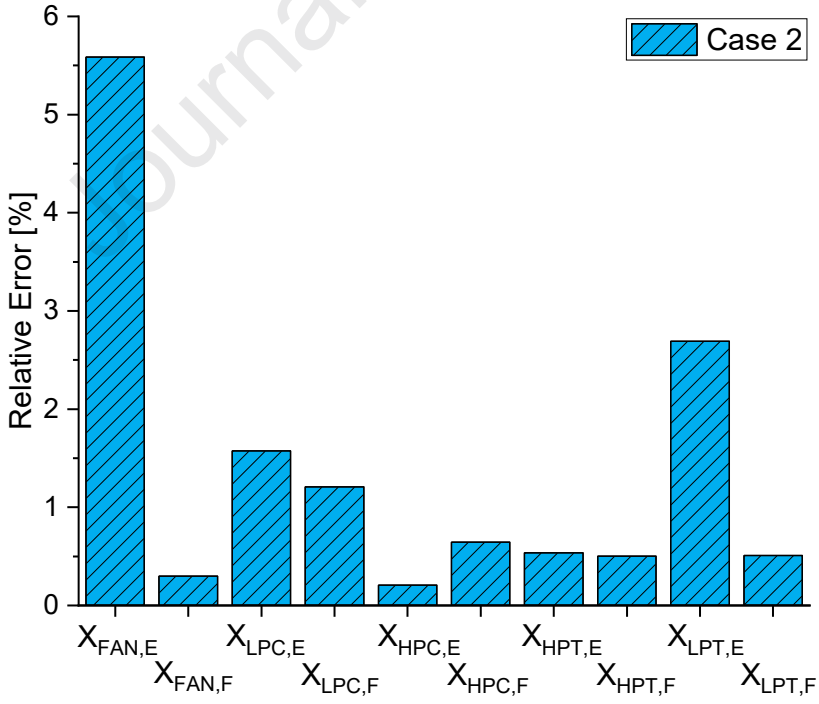

Fig. 11 Average relative error of health parameters during a transient maneuver.

3.3 Case 3: Proposed Method - Constant Health State during Transient Manoeuvre

This case study employs the proposed method for fault diagnosis during a transient maneuver while considering heat soakage in the transient engine measurements. Fig. 12 illustrates the relative error of the ten degradation indices during a dynamic maneuver.

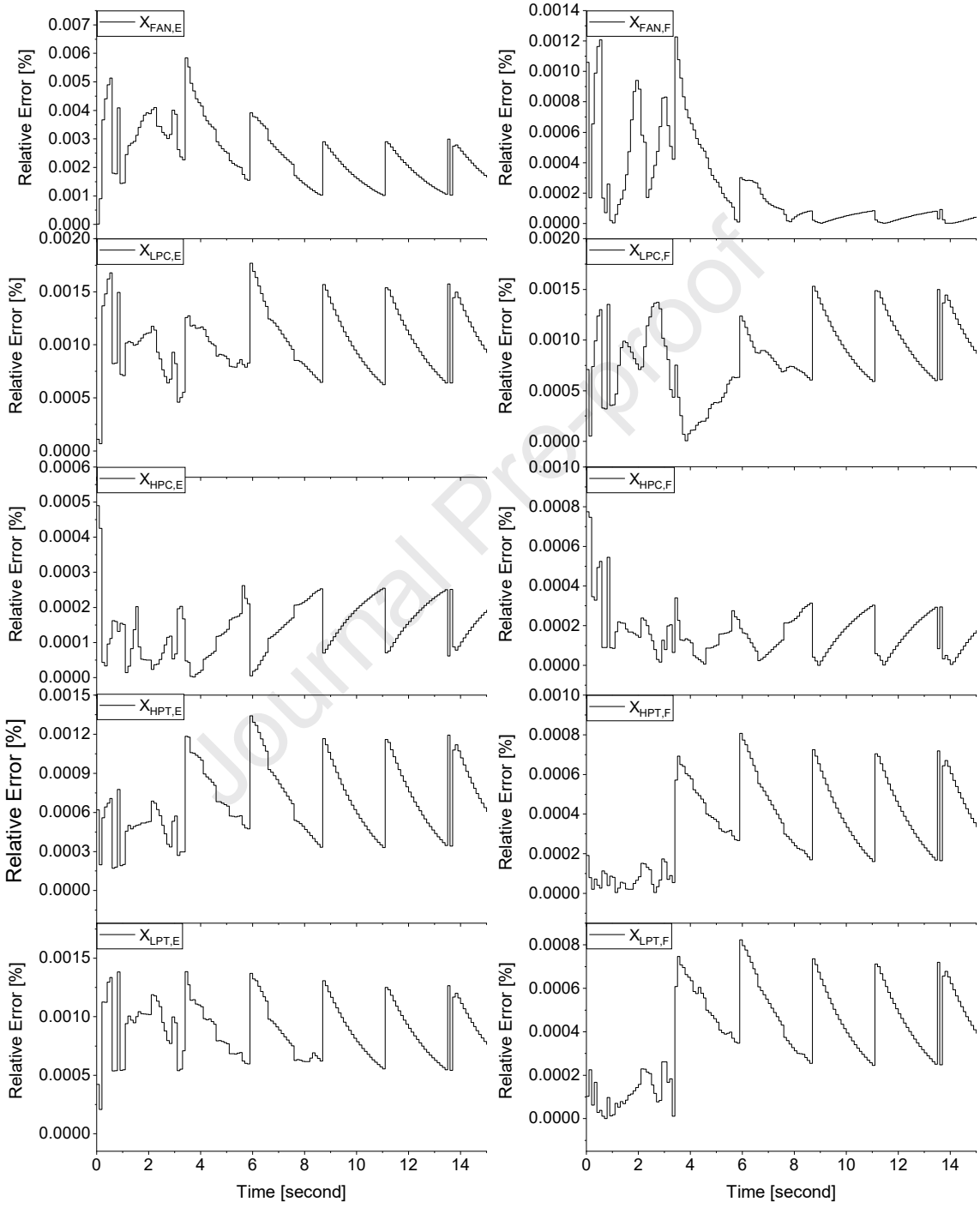

Fig. 12 Relative error of degradation indices during a dynamic maneuver.

Journal Pre-proof

Comparing the results in three cases (Fig. 13) reveals that the proposed method could estimate the health parameters with greater precision than the benchmark method. Table 4 summarises the diagnostic results for all three case studies. The computation time of Case 3 is 0.1567 s which is slightly better than that of Case 2. This is because the maximum allowed iteration steps terminate the diagnostic process; rather than the convergence threshold when affected by surplus power, heat soakage, and lag response during a transient maneuver. The average diagnostic error by the proposed method is 0.0007 % which is superior to the benchmark method (1.5239 % in Case 2). Moreover, the maximum error during the entire transient maneuver is 13.3647 % and 0.0058 % in Cases 2 and 3, respectively. It follows that the proposed time-series fault diagnosis method is superior to the benchmark method in both computational time and prediction accuracy aspects.

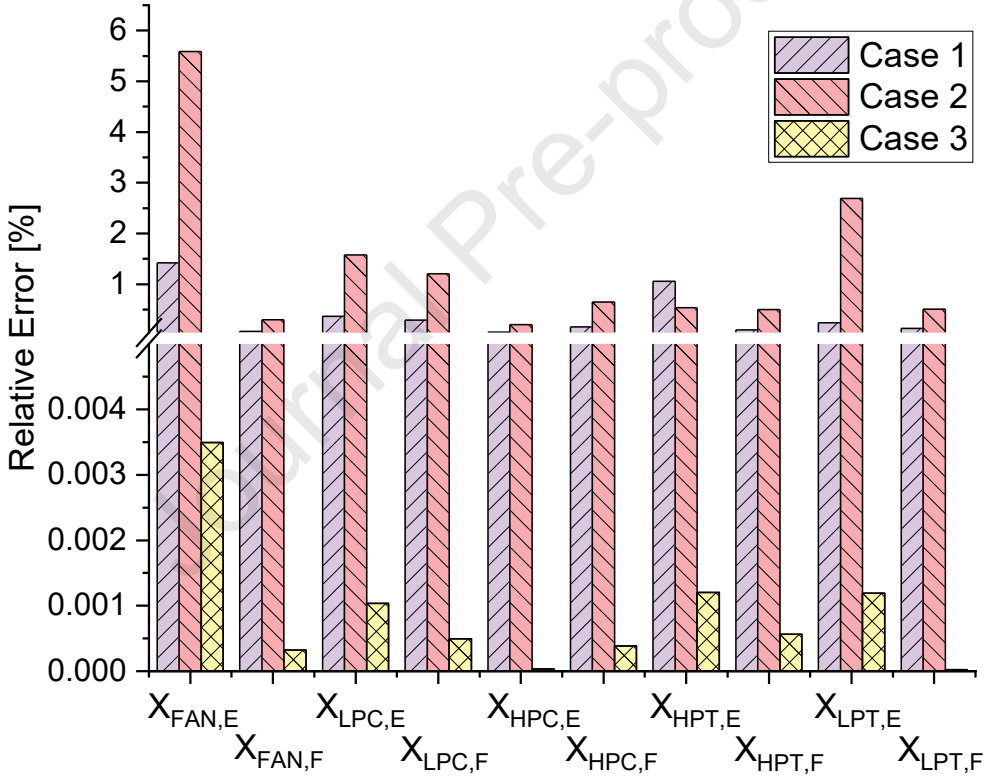

Fig. 13 Comparison of diagnosis effectively of three cases.

Table 4 Summary of three diagnosis cases.

Parameter	Symbol	Unit	Case 1	Case 2	Case 3
Average Run Time	RT	Second	0.2024	0.1997	0.1567
Average Error	AE	%	0.4224	1.5239	0.0007
Maximum Error	ME	%	6.3396	13.3647	0.0058

Journal Pre-proof

3.4 Case 4: Proposed Method - Sudden Failure during Transient Manoeuvre

The aero-engine may be faced with foreign object damage like bird strikes during flight. In such a condition, sudden degradation may happen during the flight. Moreover, the bird strike is more likely to occur during the take-off and landing processes when the engine runs under a transient or quasi-steady-state condition. Hence, it is necessary to verify the capability of the proposed method under sudden failure during dynamic conditions in real-time.

The sudden failure is assumed to happen at the 3.0 s mark during the transient maneuver in Fig. 6 (top). The health state is suddenly changed from 'Health State 1' to 'Health State 2' represented in Table 3. Fig. 14 presents the relative error of diagnostic results obtained from the proposed method during dynamic conditions with sudden failure. It can be seen from Fig. 14 that the proposed method could capture the sudden failure with high prediction accuracy. Fig. 15 compares the results of ten health parameters among all four Cases. The maximum relative error of all ten degradation indices is less than 0.0059 % in Case 4. It is evident that the relative error of all health parameters with sudden failure in Case 4 is similar to that of Case 3.

Table 5 presents the diagnostic results of all four Cases. The average computation time of Case 4 is only 0.1582 s which amplifies the suitability of the proposed method for real-time implementation. It is worth noting that the computation time of Case 4 is similar to Case 3. The sudden failure does not affect the computational efficiency of the proposed method. From the perspective of diagnostic accuracy, the average and maximum errors for all ten health parameters during the dynamic maneuver are 0.0009 % and 0.0059 %, respectively. The maximum error is observed at 3.6 s for $X_{FAN,E}$ and the sudden failure is taking place at 3.0 s, which means that the proposed algorithm is not compromised when dealing with sudden failures. The average and maximum errors of Case 4 are similar to those of Case 3. The sudden failure during the dynamic condition also does not affect diagnostic accuracy.

In summary, the results demonstrate and illustrate that the proposed method is capable of diagnosing the engine health state with time-series data at both steady-state and dynamic conditions in real-time, even when there are sudden faults during transient conditions.

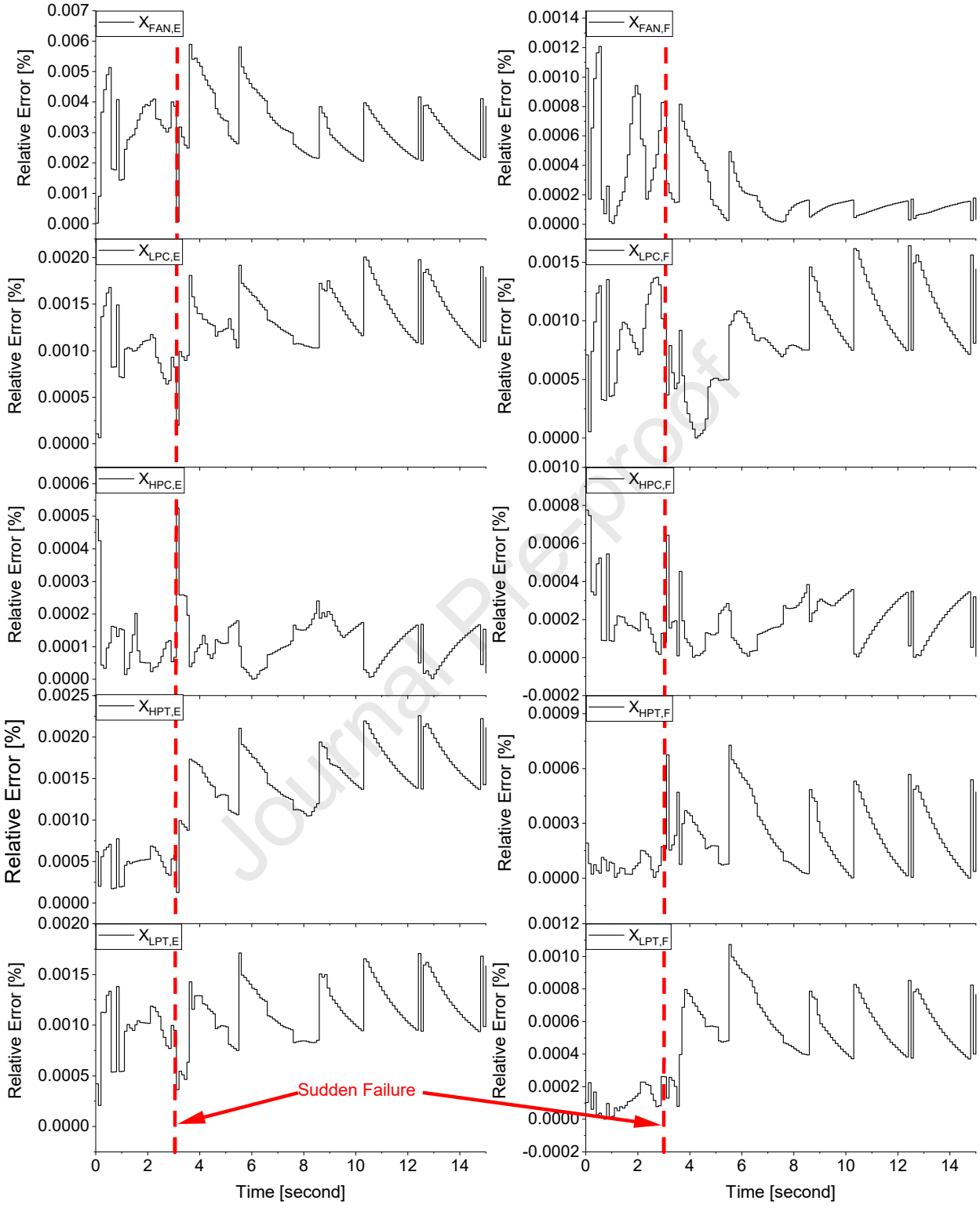

Fig. 14 Relative error of degradation indices during dynamic maneuver.

Journal Pre-proof

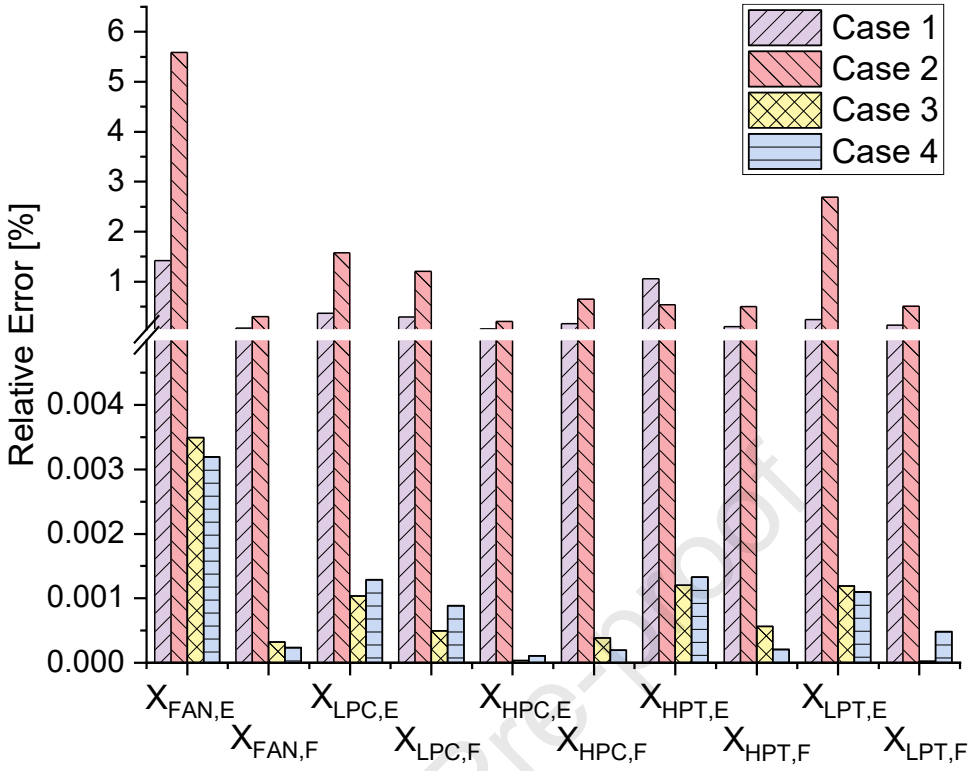

Fig. 15 Comparison of diagnosis effectively of four cases.

Table 5 Summary of four diagnostics cases.

Parameter	Symbol	Unit	Case 1	Case 2	Case 3	Case 4
Average Run Time	RT	Second	0.2024	0.1997	0.1567	0.1582
Average Error	AE	%	0.4224	1.5239	0.0007	0.0009
Maximum Error	ME	%	6.3396	13.3647	0.0058	0.0059

Despite the dynamic effect of rotor inertia, heat soakage and lag response during transient maneuver, the volume dynamic does not engage with the proposed method which may affect the diagnostic precision when very small-time step is selected. The volume dynamic is suggested to be considered in future work. However, it is worth noting that the effect of volume dynamics is less important when compared with the three dynamic effects mentioned in this study unless a limited time step is employed in the diagnostic system. Moreover, Further studies are suggested to integrate the proposed method with the aircraft and gas turbine starting models to track the engine health state from engine start until engine shut down during the whole aircraft mission. The health monitoring system could provide a real fault diagnosis in real-time on-wing, improving aircraft engine reliability, availability, and safety in such a condition.

Journal Pre-proof

4. Conclusions

This study is designed to provide the first systematic account of aero-engine transient characteristics during fault diagnosis in time-series data to fill the research gap in engine fault diagnosis under dynamic conditions. The findings clearly indicate that the proposed method could accurately diagnose the engine fault level under dynamic conditions. The most prominent finding to emerge from this study is that the sudden failure during transient conditions could be quantified correctly in real-time. In general, this study strengthens the idea that the proposed method could address the fault diagnosis of aero-engine in real-time under both stable and dynamic conditions.

The conclusions extracted from this study are below:

- When the heat soakage phenomenon during a dynamic condition is not considered, the diagnosis results predicted by the benchmark method come with a maximum error of 6.3396 %. Moreover, the predicted degradation indices fluctuate during a transient maneuver.
- The maximum diagnostic error has increased to 13.3647 during the entire transient maneuver when considering the heat soakage phenomenon in engine gas path measurements. It is clear to see that the benchmark method cannot provide correct results for the test cases.
- The proposed method could take both surplus power, heat soakage, and lag response into consideration. The maximum error of the health parameter is only 0.0058 % under a constant health state during transient conditions with a computation time of 0.1567 s.
- More importantly, the proposed method could also diagnose the sudden failure during transient maneuvers with a maximum error of 0.0059 % in 0.1582 s.

Before this study, the challenging real-time determination of the aero-engine fault level in dynamic conditions had not been investigated in detail. The present study extends our knowledge of turbofan engine fault diagnosis under dynamic conditions. A key strength of the present study is the fault diagnosis of sudden failure under transient maneuvers.

Overall, the findings of this investigation complement those of earlier studies of engine fault diagnosis under dynamic maneuvers in real-time. These findings contribute in several ways to our understanding of aero-engine fault diagnosis and benefit engine safety, availability, and reliability.

Acknowledgments

This work is supported by "the Fundamental Research Funds for the Central Universities" under Grant No. D5000220161. The authors acknowledge the support of the Propulsion and Space Research Center (PSRC) of the Technology Innovation Institute (TII) in Abu Dhabi, United Arab Emirates.

References

[1] Balli O, Caliskan H. Turbofan engine performances from aviation, thermodynamic and environmental perspectives. Energy 2021;232:121031.
[2] Sun R, Shi L, Yang X, Wang Y, Zhao Q. A coupling diagnosis method of sensors faults in gas turbine control system. Energy 2020;205:117999.
[3] Ibrahem IMA, Akhrif O, Moustapha H, Staniszewski M. Nonlinear generalized predictive controller based on ensemble of NARX models for industrial gas turbine engine. Energy 2021;230:120700.
[4] Kiaee M, Tousi AM. Vector-based deterioration index for gas turbine gas-path prognostics modeling framework. Energy 2021;216:119198.
[5] Urban LouisA. Gas Turbine Engine Parameter Interrelationships. 2nd ed. Hamilton Standard Division of United Aircraft Corporation; 1969.
[6] Volponi AJ, Tang L. Improved Engine Health Monitoring Using Full Flight Data and Companion Engine Information. SAE Int J Aerosp 2016;9:91–102.
[7] Tahan M, Tsoutsanis E, Muhammad M, Abdul Karim ZA. Performance-based health monitoring, diagnostics and prognostics for condition-based maintenance of gas turbines: A review. Applied Energy 2017;198:122–44.
[8] Li YG. A gas turbine diagnostic approach with transient measurements. Proceedings of the Institution of Mechanical Engineers, Part A: Journal of Power and Energy 2003;217:169–77.
[9] Ogaji SOT, Li YG, Sampath S, Singh R. Gas Path Fault Diagnosis of a Turbofan Engine From Transient Data Using Artificial Neural Networks. Volume 1: Turbo Expo 2003, Atlanta, Georgia, USA: ASMEDC; 2003, p. 405–14.
[10] Tsoutsanis E, Meskin N, Benammar M, Khorasani K. Transient gas turbine performance diagnostics through nonlinear adaptation of compressor and turbine maps. Journal of Engineering for Gas Turbines and Power 2015;137:1–12.
[11] Tsoutsanis E, Meskin N, Benammar M, Khorasani K. A dynamic prognosis scheme for flexible operation of gas turbines. Applied Energy 2016;164:686–701.
[12] Tsoutsanis E, Meskin N. Derivative-driven window-based regression method for gas turbine performance prognostics. Energy 2017;128:302–11.
[13] Chen Y-Z, Tsoutsanis E, Xiang H-C, Li Y-G, Zhao J-J. A dynamic performance diagnostic method applied to hydrogen powered aero engines operating under transient conditions. Applied Energy 2022;317:119148.
[14] Li J, Ying Y. Gas turbine gas path diagnosis under transient operating conditions: A steady state performance model based local optimization approach. Applied Thermal Engineering 2020;170.
[15] Hu RL, Granderson J, Auslander DM, Agogino A. Design of machine learning models with domain experts for automated sensor selection for energy fault detection. Applied Energy 2019;235:117–28.
[16] Palmé T, Fast M, Thern M. Gas turbine sensor validation through classification with artificial neural networks. Applied Energy 2011;88:3898–904.
[17] Li YG. Gas turbine performance and health status estimation using adaptive gas path analysis. Journal of Engineering for Gas Turbines and Power 2010;132:1–9.
[18] Chen Y, Zhao X, Xiang H, Tsoutsanis E. A sequential model-based approach for gas turbine performance diagnostics. Energy 2021;220:119657.
[19] Verbist M. Gas path analysis for enhanced aero-engine condition monitoring and maintenance. PhD thesis, Delft University of Technology, 2017.
[20] Park Y, Choi M, Kim K, Li X, Jung C, Na S, et al. Prediction of operating characteristics for industrial gas turbine combustor using an optimized artificial neural network. Energy 2020;213:118769.
[21] Chen Y-Z, Li Y-G, Tsoutsanis E, Newby M, Zhao X-D. Techno-economic evaluation and optimization of CCGT power Plant: A multi-criteria decision support system. Energy Conversion and Management 2021;237:114107.
[22] Wei Z, Zhang S, Jafari S, Nikolaidis T. Self-enhancing model-based control for active transient protection and thrust response improvement of gas turbine aero-engines. Energy 2022;242:123030.
[23] Pang S, Li Q, Feng H. A hybrid onboard adaptive model for aero-engine parameter prediction. Aerospace Science and Technology 2020;105:105951.
[24] Tsoutsanis E, Hamadache M, Dixon R. Real-Time Diagnostic Method of Gas Turbines Operating Under Transient Conditions in Hybrid Power Plants. Journal of Engineering for Gas Turbines and Power 2020;142:101002.

[25] Chatterjee S, Litt JS. Online model parameter estimation of jet engine degradation for autonomous propulsion control. AIAA Guidance, Navigation, and Control Conference and Exhibit, Austin, Texas, USA: 2003, p. 1–17.
[26] Chen YZ, Li YG, Newby MA. Performance simulation of a parallel dual-pressure once-through steam generator. Energy 2019;173:16–27.
[27] Park Y, Choi M, Choi G. Fault detection of industrial large-scale gas turbine for fuel distribution characteristics in start-up procedure using artificial neural network method. Energy 2022;251:123877.
[28] Hu Y, Sun Z, Cao L, Zhang Y, Pan P. Optimization configuration of gas path sensors using a hybrid method based on tabu search artificial bee colony and improved genetic algorithm in turbofan engine. Aerospace Science and Technology 2021;112:106642.
[29] Zheng J, Chang J, Ma J, Yu D. Modeling and analysis of windmilling operation during mode transition of a turbine-based-combined cycle engine. Aerospace Science and Technology 2021;109:106423.
[30] Mohammadian PK, Saidi MH. Simulation of startup operation of an industrial twin-shaft gas turbine based on geometry and control logic. Energy 2019;183:1295–313.
[31] Seyam S, Dincer I, Agelin-Chaab M. Investigation of two hybrid aircraft propulsion and powering systems using alternative fuels. Energy 2021;232:121037.
[32] Sheng H, Chen Q, Li J, Jiang W, Wang Z, Liu Z, et al. Research on dynamic modeling and performance analysis of helicopter turboshaft engine's start-up process. Aerospace Science and Technology 2020;106:106097.
[33] Wang C, Li YG, Yang BY. Transient performance simulation of aircraft engine integrated with fuel and control systems. Applied Thermal Engineering 2017;114:1029–37.
[34] Singh R, Maity A, Nataraj PSV. Dynamic modeling and robust nonlinear control of a laboratory gas turbine engine. Aerospace Science and Technology 2022:107586.
[35] Kim S. A new performance adaptation method for aero gas turbine engines based on large amounts of measured data. Energy 2021;221:119863.
[36] Collins JM, McLarty D. All-electric commercial aviation with solid oxide fuel cell-gas turbine-battery hybrids. Applied Energy 2020;265:114787.
[37] Kim MJ, Kim TS, Flores RJ, Brouwer J. Neural-network-based optimization for economic dispatch of combined heat and power systems. Applied Energy 2020;265:114785.
[38] Li Z, Li Y-G, Sampath S. Aeroengine transient performance simulation integrated with generic heat soakage and tip clearance model. Aeronaut j 2022:1–23.
[39] Tsoutsanis E, Meskin N. Dynamic performance simulation and control of gas turbines used for hybrid gas/wind energy applications. Applied Thermal Engineering 2019;147:122–42.
[40] Wei Z, Jafari S, Zhang S, Nikolaidis T. Hybrid Wiener model: An on-board approach using post-flight data for gas turbine aero-engines modelling. Applied Thermal Engineering 2021;184:116350.

Journal Pre-proof

Journal Pre-proof

Highlights

- A novel real-time successive fault diagnosis method is proposed.
- Time-series data consider the transient effect in gas path measurements.
- Constant engine degradation could be monitored with high accuracy in real-time.
- Sudden failure during dynamic conditions could be captured with great precision.
- The proposed method is far better than the benchmark method.

(maximum 85 characters, including spaces, per bullet point, 3-5 bullet points)

Journal Pre-proof

Journal Pre-proof

Declaration of interests

☑ The authors declare that they have no known competing financial interests or personal relationships that could have appeared to influence the work reported in this paper.

☐ The authors declare the following financial interests/personal relationships which may be considered as potential competing interests:

Journal Pre-proof

https://dspace.org/

A time-series turbofan engine successive fault diagnosis under both steady-state and dynamic conditions

Chen, Yu-Zhi; Tsoutsanis, Elias; Wang, Chen; Gou, Lin-Feng; Nikolaidis, Theoklis

2022-10-29
Elsevier
https://doi.org/10.1016/j.energy.2022.125848
Chen Y-Z, Tsoutsanis E, Wang C, et al., (2023) A time-series turbofan engine successive fault diagnosis under both steady-state and dynamic conditions. Energy, Volume 263, Part D, January 2023, Article number 125848

Downloaded from a DSpace repository. https://dspace.org/